ChemPubSoc Europe

DOI: 10.1002/chem.201504900

CHEMISTRY A European Journal Full Paper

Phosphanes

Synthesis and Rearrangement of *P*-Nitroxyl-Substituted P^{III} and P^{V} Phosphanes: A Combined Experimental and Theoretical Case Study

Tobias Heurich,[a] Zheng-Wang Qu,[b] Senada Nožinović,[a] Gregor Schnakenburg,[a] Hideto Matsuoka,[c] Stefan Grimme,*[b] Olav Schiemann,*[c] and Rainer Streubel*[a]

Dedicated to Professor W. W. Schoeller on the occasion of his 75th birthday

Abstract: Low-temperature generation of *P*-nitroxyl phosphane **2** ($Ph_2POTEMP$), which was obtained by the reaction of Ph_2PH (**1**) with two equivalents of TEMPO, is presented. Upon warming, phosphane **2** decomposed to give *P*-nitroxyl phosphane *P*-oxide **3** ($Ph_2P(O)OTEMP$) as one of the final products. This facile synthetic protocol also enabled access to *P*-sulfide and *P*-borane derivatives **7** and **13**, respectively, by using $Ph_2P(S)H$ (**6**) or $Ph_2P(BH_3)H$ (**11**) and TEMPO. Phosphane sulfide **7** revealed a rearrangement to phosphane oxide **8** ($Ph_2P(O)STEMP$) in $CDCl_3$ at ambient temperature, whereas in THF, thermal decomposition of sulfide **7** yielded salt **10** ($[TEMP\text{-}H_2][Ph_2P(S)O]$). As well as EPR and detailed NMR kinetic studies, indepth theoretical studies provided an insight into the reaction pathways and spin-density distributions of the reactive intermediates.

Introduction

Stable nitroxides[1] (also called nitroxyls or aminoxyls), such as TEMPO (2,2,6,6-tetramethylpiperidin-1-oxyl), have attracted interest in the last decades in molecular as well as polymer synthesis. In the latter, the interest has focused on the reversible deactivation radical polymerization (better known as living free radical polymerization).[2a,b] Specifically, the nitroxide-mediated polymerization (NMP)[2c,d] is used widely, which takes advantage of the persistent radical effect.[3] In the thermally stimulated and reversible C–O bond homolysis of an alkoxy-amine of type **I** (E = C; Scheme 1), C-centered radicals are generated, which enables various fundamental radical reactions that are based on carbon and nitroxide radicals.

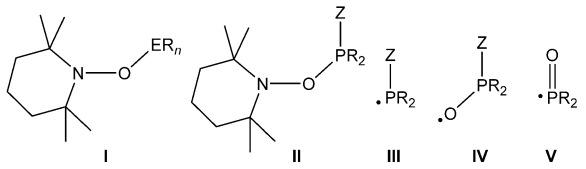

Scheme 1. O-bound main-group element derivatives of TEMPO (**I**), related phosphorus derivatives (**II**) (R = organic substituent, Z = electron pair or ML_n for a transition-metal complex fragment), and different phosphorus-containing radicals (**III**–**V**).

Besides carbon, other *p*-block element incorporated into the ER_n unit form compounds with TEMPO **I**[4] (Scheme 1), but only very few examples of *P*-nitroxyl substituted phosphanes ("*P*-TEMPO") and P^{III} derivatives **II** (Z = electron pair) are known. For example, one such intermediate was recently proposed to be formed in the reaction of diphenylphosphane with TEMPO, which was followed by homolytic O–N bond cleavage; after aqueous workup, 2,2,6,6-tetramethylpiperidinium diphenylphosphinate was obtained.[5] For other derivatives that have the formula $RR'NOPR''_2$ it was also proposed that rearrangement occurs in a similar manner, but no clear-cut evidence was provided.[6] Only in the case of perfluorinated substituents, such as CF_3 groups bound to phosphorus and nitrogen, does a *P*-nitroxyl-substituted phosphane become isolable; isomerization proceeds under harsh thermal conditions (100 °C, 42 h) to yield the aminophosphane *P*-oxide.[6a] Very recently, the reactions of a stable phosphinyl radical **III** (Z = electron pair) with different nitroxides, including TEMPO, were reported,[7] and a *P*-TEMPO-substituted phosphane **II** (Z = electron pair) was

[a] *T. Heurich, Dr. S. Nožinović, Dr. G. Schnakenburg, Prof. Dr. R. Streubel*
Institut für Anorganische Chemie
Rheinische Friedrich-Wilhelms-Universität Bonn
Gerhard-Domagk-Str. 1, 53121 Bonn (Germany)
E-mail: r.streubel@uni-bonn.de

[b] *Dr. Z.-W. Qu, Prof. Dr. S. Grimme*
Mulliken Center for Theoretical Chemistry
Rheinische Friedrich-Wilhelms-Universität Bonn
Beringstr. 4, 53115 Bonn (Germany)
E-mail: grimme@thch.uni-bonn.de

[c] *Dr. H. Matsuoka, Prof. Dr. O. Schiemann*
Institut für Physikalische und Theoretische Chemie
Rheinische Friedrich-Wilhelms-Universität Bonn
Wegelerstr. 12, 53115 Bonn (Germany)
E-mail: schiemann@pc.uni-bonn.de

Supporting information for this article can be found under: http://dx.doi.org/10.1002/chem.201504900.

again proposed as the intermediate, which after homolytic O–N bond cleavage, generated a phosphinoyl[8] (**V**) and an aminyl radical. Some chemical evidence for the former was obtained through a silyl migration to give an *O*-silyl phosphinate derivative.

Concerning transition-metal-ligated *P*-TEMPO derivatives, the knowledge about complexes **II** ($Z=ML_n$) is scarce; that is, a stable Au^{I}[9] and a thermally unstable W^0 complex have been reported so far.[10] For the latter, some evidence was obtained that, during synthesis and decomposition, radicals are involved and O–N bond homolysis seemed to be preferred, which leads to transient (and still unknown) phosphanoxyl complexes **IV** (Scheme 1).

After reviewing this background of singular and very strayed findings on the quest of O–N bond homolysis in such P^{III} compounds, it appeared interesting to develop an easily accessible system **II** that enables broad studies, of which the preliminary results will be reported herein.

Results and Discussion

When diphenylphosphane (**1**) reacted with two equivalents of TEMPO (Scheme 2), *P*-nitroxyl phosphane **2** was obtained as the intermediate at low temperature. Upon warming, it started to disappear from the reaction mixture, as evidenced by $^{31}P\{^1H\}$ NMR spectroscopy, and phosphane oxide **3** was formed

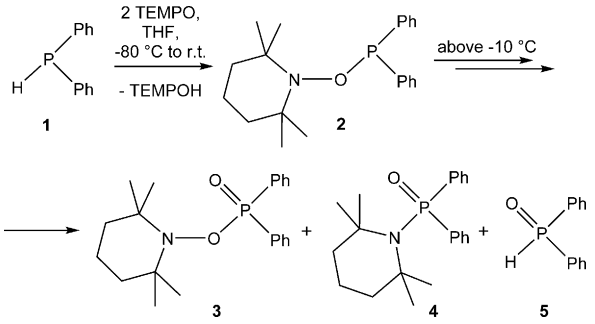

Scheme 2. Generation of phosphane **2** and its decomposition products **3**–**5**.

as the major product (90% yield) together with the two minor products **4**[11] (6% yield) and diphenylphosphane oxide **5** (4% yield by NMR integration). By using column chromatography, phosphane oxide **3** was obtained as a colorless powder in 76% yield and showed a $^{31}P\{^1H\}$ resonance at 34.0 ppm ($^1J_{P,C}=$ 135.0 Hz); the data for phosphane oxide **3** are in agreement which those reported.[12] The molecular constitution of phosphane oxide **3** was confirmed by single-crystal X-ray diffraction (Figure 1). The P–O and O–N bond lengths are 1.6081(17) and 1.481(2) Å, respectively, which are significantly shorter than a similarly substituted gold phosphane complex (*d*(P–O) 1.6314(27) and *d*(O–N) 1.4900(49) Å),[9] whereas the bond angle sum at phosphorus is slightly increased (310.8° vs. 308.3°).

As the route of formation of phosphane oxide **3** (and the other products) was not obvious, we monitored the reaction by $^{31}P\{^1H\}$ NMR spectroscopy at low temperature (Figure 2) to

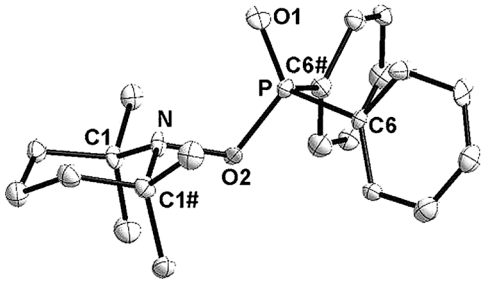

Figure 1. Molecular structure of phosphane oxide **3** (50% probability level; hydrogen atoms are omitted for clarity). Selected bond lengths in Å and angles in °: O1–P 1.4700(18), O2–P 1.6081(17), N–O2 1.481(2), C6–P 1.8091(16), C6#–P 1.8092(16), C1–N 1.4934(18), C1#–N 1.4935(18), O1-P-O2 119.43(10), C6-P-O1 112.52(7), C6#-P-O1 112.52(7), N-O2-P 117.45(13), O2-P-C6 103.11(7), O2-P-C6# 103.11(7), C16-P-C10 104.61(11).

detect intermediates. Therefore, a $[D_8]$THF solution of diphenylphosphane (**1**) and two equivalents of TEMPO was monitored initially at −80 °C, and subsequently, the temperature was increased in steps of 10 °C. In the course of the measurement, ^1H as well as $^{31}P\{^1H\}$ NMR spectra were recorded at each step. At −80 °C, two very broad signals were observed at higher field compared with substrate **1** and at lower field with respect to intermediate **2**. At most temperatures, the signals appeared as sharp lines except for the measurement at −50 °C, at which broadened signals together with sharp signals were detected again. The results clearly show the initial formation of *P*-TEMPO-substituted phosphane **2**, which starts to decompose above −10 °C to give final products **3**–**5**. We could not isolate intermediate **2**, but unambiguous NMR characterization was achieved at −20 °C; the $^{31}P\{^1H\}$ NMR resonance at 110.8 ppm revealed satellites to the *ipso*-carbon of the phenyl group ($^1J_{P,C}=23.2$ Hz; see the Supporting Information).

Furthermore, we carried out NMR kinetic studies together with theoretical calculations on the reaction mechanism. Reactions with one, two, and four equivalents of TEMPO were monitored by $^{31}P\{^1H\}$ NMR at 15 °C in real time (Table 1). Analysis of the reaction speed by differential method (Figure 3)

Table 1. Ratio (by $^{31}P\{^1H\}$ NMR integration) of reaction products and starting material for the reaction of phosphane **1** with TEMPO in $[D_8]$THF at 15 °C at the end of the reaction; $c_0(\mathbf{1})=0.3$ mol L^{-1}.

Equiv of TEMPO	**1**	**2**	**3**	**4**	**5**
1	32%	1%	43%	5%	20%
2	2%	2%	84%	10%	2%
4	–	–	94%	6%	–

yielded the rate constants, which are shown in Table 2 and Scheme 3 (for the rate laws, see the Supporting Information). The hydrogen abstraction of diphenylphosphane (**1**) by TEMPO follows a second order rate law, whereas homolytic O–N bond cleavage of intermediate **2** is a first order reaction. The first step in the reaction is most likely the rate-determining step.

The kinetic data suggest that product **4** is formed after homolytic bond cleavage, as long as the radicals are in the sol-

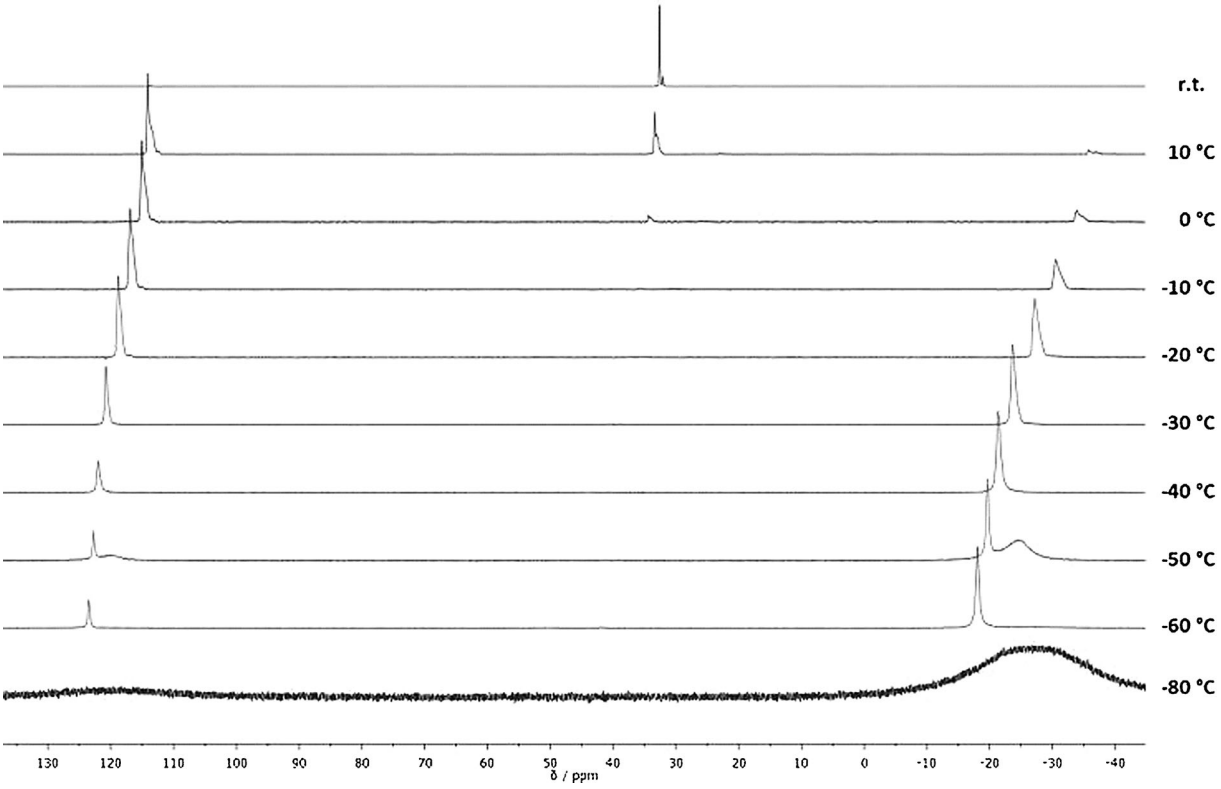

Figure 2. $^{31}P\{^{1}H\}$ NMR spectra of the reaction of diphenylphosphane **1** with TEMPO in $[D_8]$THF (low-temperature monitoring).

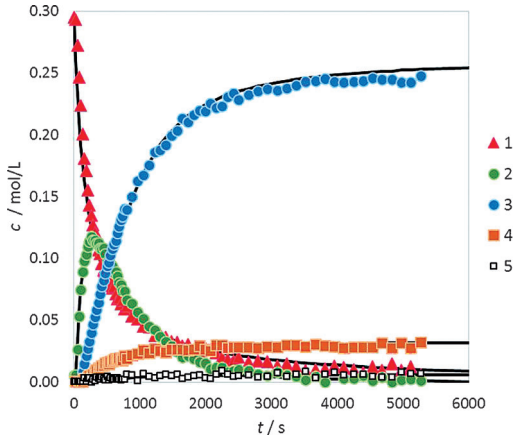

Figure 3. Time dependency of the concentration of compounds involved in the reaction of phosphane **1** with two equivalents of TEMPO at 15 °C (dots and lines represent the experimental data and the simulated values, respectively).

Table 2. Obtained rate constants for the reaction of phosphane **1** with TEMPO in $[D_8]$THF at 15 °C; $c_0(\mathbf{1}) = 0.3$ mol L^{-1}.

Equiv of TEMPO	k_1 [L mol^{-1} s^{-1}]	k_2 [L mol^{-1} s^{-1}]	k_3 [L mol^{-1} s^{-1}]	k_4 [L mol^{-1} s^{-1}]	k_5 [L mol^{-1} s^{-1}]
1	0.0075	0.10	0.0022	0.04	0.00020
2	0.0075	0.06	0.0020	0.09	0.00025
4	0.0070	0.04	0.0022	0.04	0.00020

Equiv of TEMPO	k_6 [L mol^{-1} s^{-1}]	k_7 [L mol^{-1} s^{-1}]	k_8 [L mol^{-1} s^{-1}]	k_9 [L mol^{-1} s^{-1}]
1	0.007	0.0002	0.05	0.0001
2	0.002	0.00015	0.05	0.0001
4	0.001	0.00006	0.05	0.0001

vent cage. Probably owing to the steric repulsion of the aminyl radical, this pathway (the reaction with radical **B**) is not preferred, despite the thermodynamic stability of product **4**. As expected, at higher concentrations of TEMPO, the reaction of phosphinoyl radical **B** to give product **3** is faster than its reaction to form the byproduct **5**, which is not dependent on the TEMPO concentration. If only one equivalent of TEMPO is present in the reaction solution, one third of the phosphane substrate is left over at the end of the reaction, whereas more phosphane oxide **5** is present.

We also followed the reaction of diphenylphosphane (**1**) and TEMPO in toluene by recording cw X-band EPR spectra at room temperature. With concentrated solutions of TEMPO (0.6 mol L^{-1}) and substrate **1** (0.3 mol L^{-1}), we initially observed an unstructured broad line; the broadening was ascribed to intermolecular exchange interactions between TEMPO molecules at this high concentration. Over time, the EPR signal decayed and a narrowing of the linewidth was observed, which resulted in the appearance of the typical hyperfine structure of TEMPO owing to the coupling with the nitrogen nucleus (Figure 4); after the mixture was left overnight at room temperature, 99.9% of the TEMPO was consumed. Overall, the EPR results

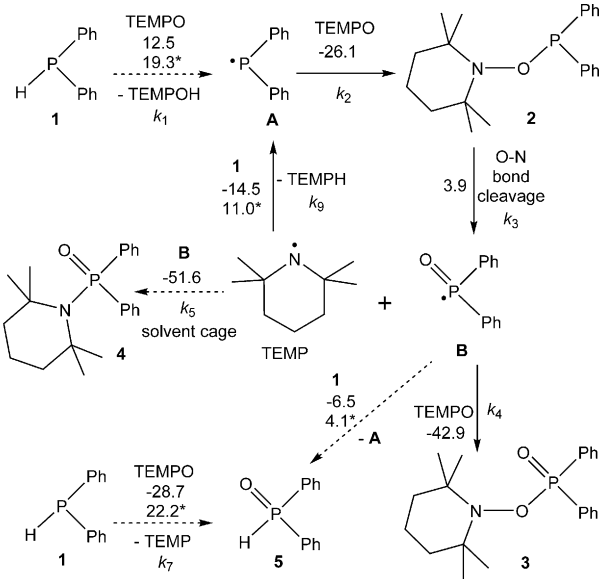

Scheme 3. The DFT-computed free-energy paths (in kcal mol^{-1}; values with * indicate barrier heights) for the reaction between diphenylphosphane **1** and TEMPO at 298 K with associated reaction rate constants. Reactions that lead to minor products are indicated by dashed arrows.

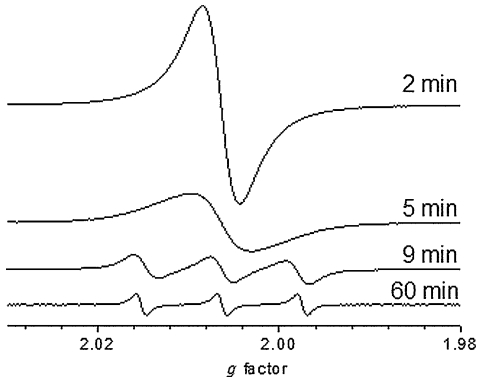

Figure 4. Room-temperature EPR spectra at 2, 5, 9, and 60 min after mixing toluene solutions of phosphane **1** and TEMPO.

clearly demonstrate that the concentration of TEMPO decays as the reaction proceeds. Unfortunately, no other radical intermediates were observed; this may be due to the intense TEMPO signal. The strong exchange broadening in turn prevents a meaningful analysis of the kinetics. Decreasing the TEMPO concentration, thus enabling a clearly resolved TEMPO spectrum, slows the reaction to such an extent that no signal decay is observed. This indicates that the TEMPO concentration plays an important role in the rate law of the reaction.

Theoretical studies of the reaction mechanism were performed in the gas phase by using the RHF framework (UHF framework used only for open-shell radicals) at the TPSS-D3/def2-TZVP level of theory,[13–18] which is sufficiently accurate (typically within 2 kcal mol^{-1}) for various reactions that involve only neutral species in weakly polar solvents, such as THF. As the P–H bond in phosphane **1** is about 12 kcal mol^{-1} weaker than the C–H bonds in a THF molecule, selective H-abstraction from **1** (rather than from solvent) by radical intermediates was expected, which is also consistent with the above experimental observations. As shown in Scheme 3, the initial H-abstraction by O···H–P attack between the TEMPO radical and diphenylphosphane **1** is endergonic by 12.5 kcal mol^{-1} and proceeds over a moderate free-energy barrier of 19.3 kcal mol^{-1} to give the reactive diphenylphosphanyl radical **A**, which can be easily quenched by excess TEMPO in an exergonic step (−26.1 kcal mol^{-1}) to form the *P*-nitroxyl phosphane intermediate **2**. On the other hand, direct O atom transfer from TEMPO by O···P attack is exergonic by −28.7 kcal mol^{-1}, but it has a higher free-energy barrier of 22.2 kcal mol^{-1} to form diphenylphosphane oxide **5**, which is thus kinetically less competitive, as confirmed by the 40-fold smaller experimental rate constant k_7 (see the Supporting Information). The estimated rate constants at 15 °C of 0.03 and 0.0002 L mol^{-1} s^{-1} for k_1 and k_7, respectively, were determined by using traditional transition-state theory and are reasonably consistent with the experimental ones. Our DFT calculations show that the initial H-abstraction from phosphane **1** by TEMPO is the rate-limiting step. Other reaction steps have much lower energy barriers or are even barrierless and could be limited by other facts, such as solvent cage and diffusion rates in solution. The intermediate **2** is thermally unstable with respect to the O–N bond cleavage, which is endergonic by only 3.9 kcal mol^{-1} and leads to the formation of diphenylphosphinoyl radical **B** and reactive radical TEMP (2,2,6,6-tetramethylpiperidinyl). The radical **B** shows delocalized spin density that is mainly on the P (0.51 *e*) and the O (0.27 *e*) atoms (Figure 8). This intermediate can be easily quenched by other radical species present, such as TEMPO and TEMP (minor), to form the experimentally observed major and minor product **3** and **4**, respectively. On the other hand, H-abstraction of phosphane **1** by radical **B** (and minor TEMPOH) can easily lead to diphenylphosphane oxide **5** as the other experimentally observed minor product. The radical TEMP cannot be trapped by TEMPO through radical recombination, but it does abstract hydrogen from substrate **1** (and minor TEMPOH) easily, which leads to the observed TEMPH and the regenerated intermediate **A** for further reaction cycle.

Even though three equivalents of TEMPO would be formally required in the steps with k_1, k_2, and k_4 for the formation of the major product **3**, one equivalent of TEMPO is saved by the reactive radical intermediate TEMP from the step with k_3 by either TEMPO recycling from the TEMPOH intermediate or direct regeneration of the radical intermediate **A** to skip the initial H-abstraction step by TEMPO. Obviously, in addition to the initiating H-abstraction by TEMPO, H-abstraction from phosphane **1** by intermediate TEMP over the 7.9 kcal mol^{-1} lower free-energy barrier can be important to maintain the radical reaction cycle from the key intermediate **A** at low TEMPO concentration. Owing to the complicated competing reactions, the outcome of the reaction of **1** and TEMPO is strongly dependent on the reaction conditions, such as temperature and reactant ratio. At room temperature and high TEMPO ratio, the reaction is dominated by the trapping of radical **B** by TEMPO, which leads to the main reaction channel: **1**+2TEMPO → **3**+TEMPH.

Although phosphane oxide **3** was obtained as the major product when only one equivalent of TEMPO was used, the trapping of radical **B** by TEMPO became less efficient, and radical recombination with TEMP and H-abstraction from phosphane **1** became possible from intermediate **B**, which leads to side channels that require a smaller TEMPO ratio, such as: 2**1**+2TEMPO → **4**+**5**+TEMPH.

Having obtained the P^V oxide species **3**, which is also accessible by reacting phosphane oxide **5** with two equivalents of TEMPO, we next targeted the P^V sulfide derivative. Reaction of diphenylphosphane sulfide **6**[19] with two equivalents of TEMPO under otherwise identical conditions led to P^V sulfide **7** in an almost quantitative reaction (95% yield, Scheme 4); product **7** was purified by column chromatography (85% yield). The $^{31}P\{^1H\}$ NMR resonance of sulfide **7** appears at lower field (88.1 ppm, $^1J_{P,C}=108.7$ Hz) than phosphane oxide **3**. Single-crystal X-ray diffraction confirmed the molecular constitution of sulfide **7** (Figure 5); the P–O bond (1.6230(14) Å) and the O–N bond (1.493(2) Å) were elongated compared with phosphane oxide **3**.

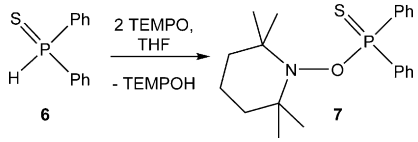

Scheme 4. Synthesis of phosphane sulfide **7**.

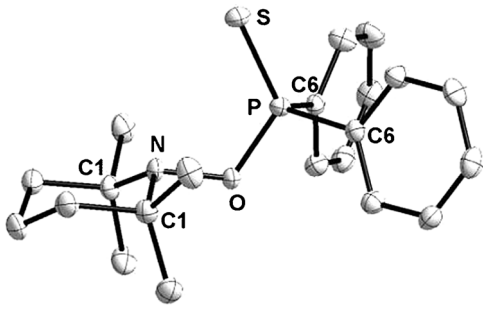

Figure 5. Molecular structure of phosphane sulfide **7** (50% probability level; hydrogen atoms are omitted for clarity). Selected bond lengths in Å and angles in °: S–P 1.9308(7), P–O 1.6230(14), O–N 1.493(2), P–C6 1.8095(16), N–C1 1.4920(18), O-P-S 118.78(6), N-O-P 117.12(11), O-P-C6 103.33(6), C6-P-S 112.55(5), C6#1-P-C6 104.90(10).

Compound **7** revealed an interesting follow-up chemistry: a slow reaction (7 days) in dry $CDCl_3$ led to a major product that displayed a resonance in the $^{31}P\{^1H\}$ NMR spectrum at 38.4 ppm ($^1J_{P,C}=98.1$ Hz). This was identified as the phosphane oxide **8** (Scheme 5), which was formed together with small amounts (≈20%) of a byproduct **9**[20,21] (two doublets at 29.4 and 80.3 ppm, $^2J_{P,P}=39.7$ Hz), which could not be isolated. Compound **8** was obtained in its pure form by column chromatography. Single-crystal X-ray analysis confirmed the structure of phosphane oxide **8** and revealed P–S and S–N bond lengths of 2.1072(4) and 1.7243(10) Å, respectively (Figure 6).

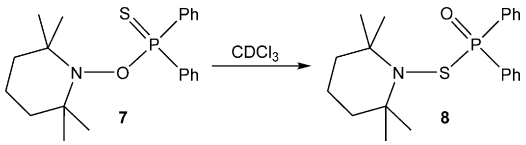

Scheme 5. Rearrangement of phosphane sulfide **7** to phosphane oxide **8**.

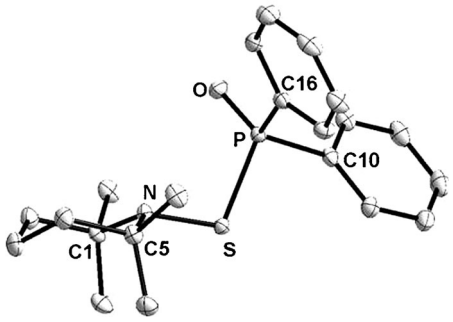

Figure 6. Molecular structure of phosphane oxide **8** (50% probability level; hydrogen atoms are omitted for clarity). Selected bond lengths in Å and angles in °: P–O 1.4831(9), P-S 2.1072(4), S–N 1.7243(10), P–C10 1.8099(12), P–C16 1.8118(12), N–C1 1.5131(15), N–C5 1.5102(15), O-P-S 117.42(4), N-S-P 104.16(4), O-P-C10 112.73(6), O-P-C16 110.56(6), C10-P-S 97.94(4), C16-P-S 109.43(4), C10-P-C16 107.83(5).

Compound **7** showed a different behavior in THF. Heating a solution to 60 °C resulted in the formation of salt **10**, which was obtained as the major product (Scheme 6); a byproduct **11**[20] (15% yield) was also observed in the $^{31}P\{^1H\}$ NMR spectrum (79.3 ppm), but could not be isolated.

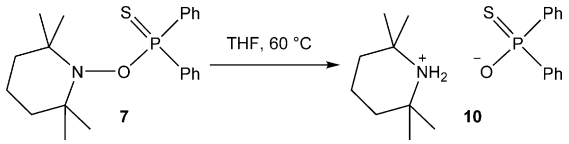

Scheme 6. Decomposition of phosphane sulfide **7** to salt **10**.

Compound **10** was purified by column chromatography to yield a colorless powder (23% yield). The $^{31}P\{^1H\}$ NMR resonance of salt **10** appeared at 52.1 ppm ($^1J_{P,C}=103.3$ Hz), which is highfield-shifted compared with sulfide **7**. Single-crystal X-ray diffraction studies confirmed the structure of salt **10** (Figure 7); separate ion pairs were shown with the oxygen atom of the anionic part pointing towards the nitrogen atom of the cationic part. The O···N distance is 2.7681(8) Å, which indicates that no covalent interaction is present between these atoms. The P–S bond length of 1.9935(9) Å indicates some double-bond character, whereas the P–O bond length of 1.5097(11) Å suggests more single-bond character.

Similar to the reaction of compound **1** with TEMPO, the detailed mechanism for the reaction between diphenylphosphane sulfide **6** and TEMPO was studied by DFT methods (Scheme 7). The initial H-abstraction through O···H–P attack by TEMPO radical is endergonic by 12.7 kcal mol^{-1} over an even lower free-energy barrier of 14.0 kcal mol^{-1} to give the reactive

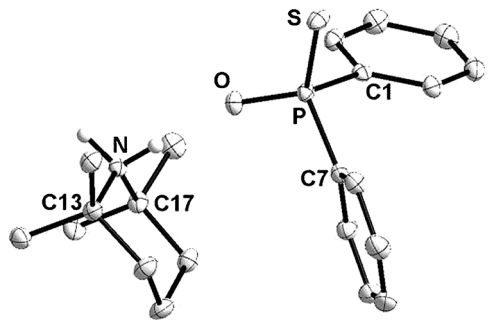

Figure 7. Molecular structure of salt **10** (50% probability level; hydrogen atoms are omitted for clarity). Selected bond lengths in Å and angles in °: P–O 1.5097(11), P–S 1.9935(9), P–C1 1.8267(16), P–C7 1.8286(16), N–C13 1.5292(19), N–C17 1.5293(18), O-P-S 117.83(5), O-P-C1 107.68(7), O-P-C7 109.67(7), C1-P-S 108.27(5), C7-P-S 108.69(5), C1-P-C7 103.78(7).

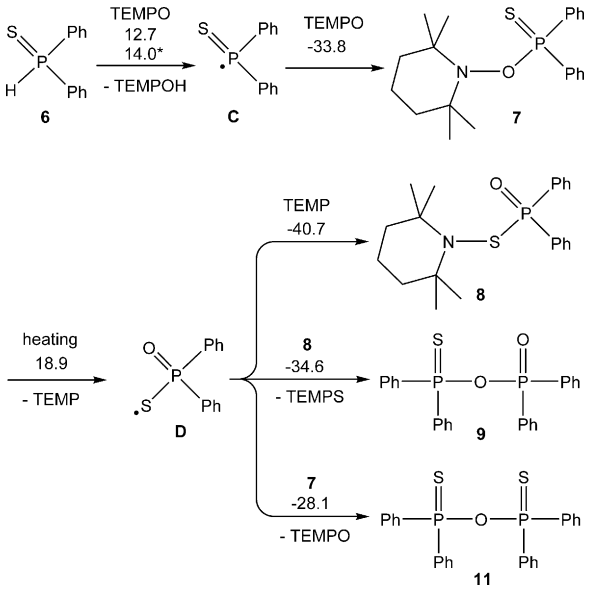

Scheme 7. The DFT-computed free-energy paths (in kcal mol^{-1}; values with * indicate barrier heights) at 298 K for the formation of compounds **7**–**11**.

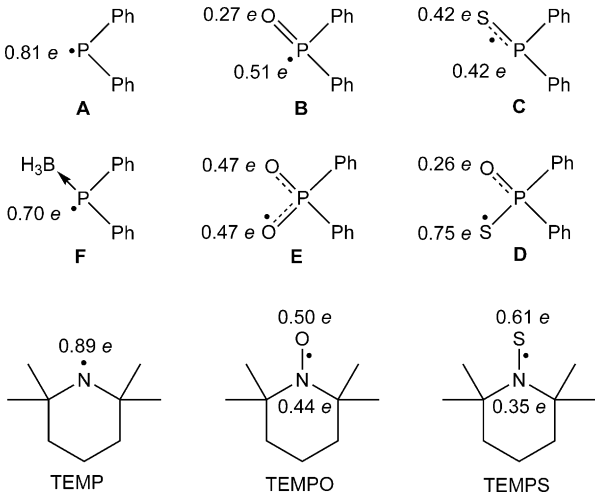

Figure 8. DFT-computed Mulliken spin densities on heavy atoms within some radical species.

radical **C**, which can be easily quenched by excess TEMPO in a −33.8 kcal mol^{-1} exergonic step to form the *P*-nitroxyl phosphane sulfide **7**. In contrast to intermediate **2**, compound **7** is thermally much more stable with respect to the O–N bond cleavage and is thus separable even at room temperature. Under normal conditions at 298 K, the O–N bond cleavage of sulfide **7** to form the radical **D** is endergonic by 18.9 kcal mol^{-1}, which is accelerated by heating, owing to favorable entropy effects (increasing entropies by bond dissociation), and by coupling with more exergonic radical quenching of reactive species **D**, which could be maintained only at very low concentration in solution. The key radical intermediate **D** shows somewhat delocalized spin densities that are mainly on the S (0.75 *e*) and the O (0.26 *e*) atoms (Figure 8). As before, this radical can be easily quenched by the eliminated TEMP radical through S–N bond formation in a highly exergonic step that leads to the experimentally observed isomerization product **8**. For the **7**→**8** rearrangement, direct shift of the bulky TEMP group between the O and S atoms is also possible, but it is kinetically less favourable over a higher free-energy barrier of 26.7 kcal mol^{-1} (see the Supporting Information). On the other hand, the O···P attacks by radical **D** at the *P*-center of compounds **7** and **8** are also highly exergonic through the formation of strong P–O bonds and simultaneous elimination of TEMPS and TEMPO radicals, which are responsible for the formation of the products **9** and **11**; these species might account for the experimentally detected minor products.

In contrast to the $(TEMP)_2O$ molecule, which is thermally unstable, the radical recombination between TEMPS and TEMP is exergonic by −14.3 kcal mol^{-1}, according to our DFT calculations, and leads to the formation of the stable $(TEMP)_2S$[22] species. When compound **7** is heated in THF, the initially formed reactive TEMP and **D** radicals can even abstract H atoms from THF in neutral or slightly exergonic steps; exergonic intermolecular proton transfer to give the TEMP–H species leads to the formation of the experimentally observed ionic product **10**, in accordance with the same thermal decomposition mechanism that has recently been established by us for a closely related *P*-nitroxyl phosphane complex.[10b]

To examine the effects of heavier chalcogen atoms that are directly bound to phosphorus, we examined a set of related phosphorus compounds with particular focus on the spin-density distribution (Figure 8). For the simplest diphenylphosphanyl radical **A**, the spin density is mainly localized on the P center (0.81 *e*). Binding BH_3 to the P center through the electron lone pair of radical **A** slightly reduces the spin density by only 0.11 *e*. Binding one O or S atom to the P center of radical **A** to form partial double bonds leads to delocalized spin densities over the P and O or P and S atoms. The spin density on the P center can be completely removed by a further O or S atom, which leads to partly localized spin densities on the termini (O and S atoms). The replacement of an O by an S atom may lead to more localized spin on the S ligand, as also seen for TEMPO.

To get further insight into the bonding and stability of different *P*-TEMPO moieties, we decided to involve the lone pair on

the phosphorus into a dative bond with borane (BH_3). First attempts to use the phosphane borane complex **12**[23] and TEMPO only showed low conversion (≈25%). It turned out that initial deprotonation of complex **12** at low temperatures and subsequent reaction with TEMPO (2 equiv) was required, which then led to the *P*-TEMPO-substituted phosphane borane complex **13** (Scheme 8) in a better selectivity (≈55% yield). Again, the molecular structure of complex **13** was confirmed by single-crystal X-ray diffraction (Figure 9); here, the P–O and

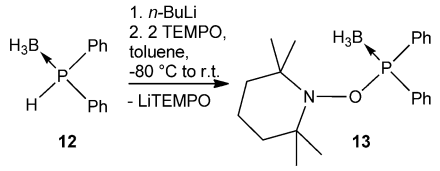

Scheme 8. Synthesis of phosphane borane complex **13**.

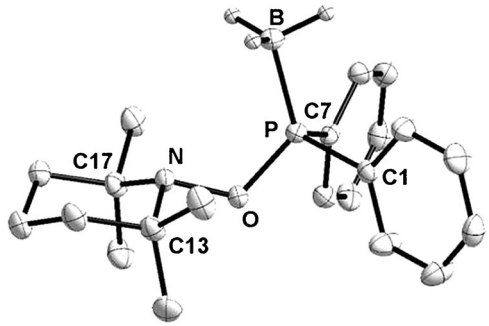

Figure 9. Molecular structure of phosphane borane complex **13** (50% probability level; hydrogen atoms are omitted for clarity). Selected bond lengths in Å and angles in °: P–O 1.6236(9), P–B 1.9017(16), O–N 1.4892(13), P–C1 1.8136(13), P–C7 1.8108(13), N–C13 1.4962(16), N–C17 1.5013(16), O–P-B 121.79(6), N-O-P 116.63(7), O-P-C1 102.25(5), O-P-C7 100.93(5), C1-P-B 111.92(7), C7-P-B 113.06(7), C1-P-C7 105.03(6).

O–N bond lengths are 1.6236(9) and 1.4892(13) Å, respectively, which are getting close to the values that have been reported previously for the gold complex.[10] Our DFT calculations suggest the same mechanism for the formation of complex **13** as for the complexes **2** and **7**, i.e., initial H-abstraction by TEMPO followed by radical trapping by another TEMPO. Interestingly, the O–N bond dissociation free energies (in kcal mol^{-1}) increase in the order: **2** (3.9) < **7** (18.9) < **13** (20.2), which clearly indicates the stabilizing role of electron-withdrawing ligands that are attached to the adjacent P center.

Conclusion

Strong NMR spectroscopic evidence for the intermediate formation of the *P*-nitroxyl phosphane **2**, which was obtained from the reaction of diphenylphosphane **1** with two equivalents of TEMPO, was presented; the radical reaction was further monitored by EPR spectroscopy. On the basis of detailed theoretical and NMR kinetic studies, a reaction pathway that leads to the final products was proposed. The same facile synthetic approach was used to access the *P*-sulfide and *P*-borane derivatives **7** and **13**, respectively, and theoretical studies provided insights into the influence of oxidation on the O–N bond dissociation free energies as well as the spin density distribution within the resulting P-containing radical species. Preliminary results on the reactivity of *P*-sulfide **7** were obtained: in $CDCl_3$, rearrangement to the *P*-oxide **8** occurred at ambient temperature, whereas in THF, thermal decomposition yielded salt **10**; the latter formally resulted from a two-fold radical H atom abstraction after O–N bond cleavage, followed by exergonic intermolecular proton transfer. Overall, this study sheds first light on the emerging chemistry of *P*-nitroxyl derivatives.

Experimental Section

All manipulations involving air- and moisture-sensitive compounds were carried out under an atmosphere of purified argon by using standard Schlenk-line techniques or a glove-box. Solvents were dried with appropriate drying agents and degassed before use. The ^{1}H, $^{13}C\{^{1}H\}$, and $^{31}P\{^{1}H\}$ NMR (δ in ppm) spectroscopic data were, if not specially noted, recorded ($CDCl_3$, 25 °C) on a Bruker DMX 300 spectrometer. Mass spectra were recorded on a MAT 95 XL Thermo Finnigan spectrometer (selected data given), and ESI mass spectra were recorded with a micrOTOF-Q of Bruker Daltonik. Infrared spectra were recorded on a Thermo Nicolet 380 FT-IR spectrometer or Bruker ALPHA (selected data given). Elemental analyses were determined with a gas chromatograph Vario EL from Elementa. Melting-point measurements were performed with an apparatus from Büchi according to Dr. Tottoli.

Diphenylphosphane **1** was purchased from abcr and used as received. Diphenylphosphane sulfide **6**[19] and diphenylphosphane borane complex **12**[23] were prepared in accordance with known literature methods. More information on NMR measurements as well as X-ray measurements and structure solution can be found in the Supporting Information.

The EPR spectra were recorded on a Bruker EMX-micro EPR spectrometer equipped with EMX standard resonator (4119HS) both from Bruker. The EPR measurements started immediately after mixing toluene solutions of **1** (0.3 mol L^{-1}) and TEMPO (0.6 mol L^{-1}) in an quartz EPR tube with an inner and outer diameter of 3 and 4 mm, respectively. EPR spectra were collected with a microwave power of 17.8 μW, a modulation frequency of 100 Hz, a modulation amplitude of 0.7 G, a microwave frequency of 9.835 GHz, and 1429 points in the field interval 345.2–355.2 mT.

The quantum chemical DFT calculations have been performed with the TURBOMOLE suite of programs[24,25] at the TPSS-D3/def2-TZVP level of theory, which combines the TPSS density functional[13] with the BJ-damped DFT-D3 dispersion correction[14,15] and the def2-TZVP basis set.[16–18] The density-fitting RI-J approach[26,27] was used to accelerate the geometry optimization and harmonic frequency calculations. All structures were fully optimized, followed by frequency analysis to identify the nature of located stationary points and to provide thermal and free-energy corrections according to the ideal gas-rigid rotor-harmonic oscillator model. The structures were characterized as true minima (with no imaginary frequency) or transition states (with only one imaginary frequency). In our discussion, the Gibbs free energies (in kcal mol^{-1}) at 298.15 K related to ideal gas under 1 atm (i.e., 0.04 mol L^{-1}) are used unless specified otherwise. For open-shell radical species, the spin densities were computed according to the Mulliken population analysis by using unrestricted (spin-polarized) Scheme.

The samples for kinetic NMR studies were prepared by using Schlenk technique. A solution of diphenylphosphane **1** (0.5 mL, 0.3 mol L^{-1}) in THF was cooled to −80 °C and then transferred by a double needle to a TEMPO solution (0.5 mL, 0.3 mol L^{-1} for 1 equiv; 0.6 mol L^{-1} for 2 equiv; 1.2 mol L^{-1} for 4 equiv) in the same solvent at the same temperature. The reaction mixture was then transferred to a cooled (−100 °C) NMR tube and immediately taken to the spectrometer for the measurement at 15 °C. The dynamics center software (Vers. 2.3.1) by Bruker BioSpin NMR was used to analyze the obtained data.

Low-temperature NMR characterization of phosphane 2

An NMR tube with a solution of TEMPO (93.8 mg, 0.3 mmol) in [D_8]THF (0.5 mL) was cooled to −80 °C (ethanol/liquid N_2 bath), and diphenylphosphane **1** (56 mg, 0.3 mmol) was added. ^{1}H NMR (300.13 MHz, [D_8]THF, −20 °C, TMS): δ = 0.9 (s, 6H, CH_3), 1.2 (s, 6H, CH_3), 1.3–1.7 (br m, 6H, CH_2-C(CH_3)$_2$ and CH_2-CH_2-CH_2), 7.2–7.4 (m, 6H, H_{Ph}), 7.5–7.7 ppm (m, 4H, H_{Ph}); ^{13}C{^{1}H} NMR (75.48 MHz, [D_8]THF, −20 °C, TMS): δ = 17.7 (s, CH_2-CH_2-CH_2), 20.1 (s, CH_3), 33.4 (s, CH_3), 40.8 (s, CH_2-C(CH_3)$_2$), 60.6 (d, $^3J_{P,C}$ = 2.3 Hz, N-C(CH_3)$_2$), 128.9 (d, $^4J_{P,C}$ = 17.6 Hz, *p*-C_{Ph}), 129.4 (d, $^3J_{P,C}$ = 36.4 Hz, *m*-C_{Ph}), 130.8 (d, $^2J_{P,C}$ = 24.3 Hz, *o*-C_{Ph}), 144.9 ppm (d, $^1J_{P,C}$ = 21.6 Hz, *ipso*-C_{Ph}); ^{31}P{^{1}H} NMR (121.51 MHz, [D_8]THF, −20 °C, H_3PO_4): δ = 110.8 ppm (s_{Sat}, $^1J_{P,C}$ = 23.2 Hz).

Synthesis of phosphane oxide 3

A solution of TEMPO (1.88 g, 12.0 mmol, 2 equiv) in THF (5 mL) was added to a stirring solution of diphenylphosphane **1** (1.12 g, 6.0 mmol) in THF (10 mL). After 18 h, volatiles were removed under reduced pressure (3×10^{-2} mbar). The residue was purified by column chromatography at −5 °C (SiO_2, h = 5 cm, $\varnothing$ = 4.5 cm; Et_2O/CH_2Cl_2 1:1). Evaporation of the solvent of the first fraction gave **3** as a colorless solid. Single crystals that were suitable for X-ray study were obtained from a saturated Et_2O solution (1.65 g, 4.5 mmol, 76%). M.p. 131 °C; ^{1}H NMR (300.13 MHz, $CDCl_3$, 25 °C, TMS): δ = 1.1 (br s, 12H, CH_3), 1.4 (br s, 1H, CH_2-CH_2-CH_2), 1.5 (br s, 5H, CH_2-C(CH_3)$_2$ and CH_2-CH_2-CH_2), 7.3–7.5 (m, 6H, H_{Ph}), 7.8–7.9 ppm (m, 4H, H_{Ph}); ^{13}C{^{1}H} NMR (75.48 MHz, $CDCl_3$, 25 °C, TMS): δ = 17.0 (s, CH_2-CH_2-CH_2), 20.6 (br s, CH_3), 33.7 (br s, CH_3), 40.2 (s, CH_2-C(CH_3)$_2$), 61.6 (d, $^3J_{P,C}$ = 2.6 Hz, NC(CH_3)$_2$), 128.3 (d, $^3J_{P,C}$ = 12.9 Hz, *m*-C_{Ph}), 131.6 (s, $^4J_{P,C}$ = 2.8 Hz, *p*-C_{Ph}), 131.7 (d, $^2J_{P,C}$ = 9.4 Hz, *o*-C_{Ph}), 134.0 ppm (d, $^1J_{P,C}$ = 135.0 Hz, *ipso*-C_{Ph}); ^{31}P{^{1}H} NMR (121.51 MHz, $CDCl_3$, 25 °C, H_3PO_4): δ = 34.0 ppm (s_{sat}, $^1J_{P,C}$ = 135.0 Hz); IR (neat): $\tilde{\nu}$ = 1229 cm^{-1} (s, P=O); MS (EI, 70 eV): *m/z* (%): 357 $[M]^{+\bullet}$ (2); elemental analysis calcd (%) for $C_{21}H_{28}NO_2P$ (357.43 g mol^{-1}): C 70.57, H 7.90, N 3.92; found: C 70.31, H 7.90, N 3.91.

Synthesis of phosphane sulfide 7

Diphenylphosphane sulfide **6** (1.2 g, 5.56 mmol) was dissolved in THF (7 mL), and a solution of TEMPO (1.74 g, 11.12 mmol) in THF (3 mL) was added. After 17 h, all volatiles were removed under reduced pressure (3×10^{-2} mbar). The residue was purified by column chromatography at −20 °C (SiO_2, h = 5 cm, $\varnothing$ = 4.5 cm, petroleum ether/Et_2O, stepwise gradient, 1:0–0:1). Evaporation of the first fraction gave sulfide **7** as a colorless solid that was recrystallized from Et_2O at −50 °C. Single crystals that were suitable for X-ray study were obtained from saturated Et_2O solution (1.763 g, 4.73 mmol, 85%). M.p. 127 °C; ^{1}H NMR (300.13 MHz, $CDCl_3$, 25 °C, TMS): δ = 1.2 (s, 12H, CH_3), 1.2–1.7 (br m, 6H, CH_2-C(CH_3)$_2$ and CH_2-CH_2-CH_2), 6.9–7.1 (m, 6H, H_{Ph}), 8.1–8.3 ppm (m, 4H, H_{Ph}); ^{13}C{^{1}H} NMR (75.48 MHz, $CDCl_3$, 25 °C, TMS): δ = 17.2 (s, CH_2-CH_2-CH_2), 21.1 (br s, CH_3), 33.7 (br s, CH_3), 40.4 (s, CH_2-C(CH_3)$_2$), 61.4 (d, $^3J_{P,C}$ = 3.0 Hz, N-C(CH_3)$_2$), 128.4 (d, $^3J_{P,C}$ = 12.7 Hz, *m*-C_{Ph}), 131.1 (d, $^4J_{P,C}$ = 2.9 Hz, *p*-C_{Ph}), 131.5 (d, $^2J_{P,C}$ = 10.0 Hz, *o*-C_{Ph}), 138.0 ppm (d, $^1J_{P,C}$ = 108.7 Hz, *ipso*-C_{Ph}); ^{31}P{^{1}H} NMR (121.51 MHz, $CDCl_3$, 25 °C, H_3PO_4): δ = 88.1 ppm (s_{Sat}, $^1J_{P,C}$ = 108.7 Hz); MS (EI, 70 eV): *m/z* (%): 373 $[M]^{+\bullet}$ (16); elemental analysis calcd (%) for $C_{21}H_{28}NOPS$ (373.49 g mol^{-1}): C 67.53, H 7.56, N 3.75, S 8.59; found: C 67.27, H 7.40, N 3.84, S 8.82.

Isolation of phosphane oxide 8

Phosphane sulfide **7** (1 g, 2.68 mmol) was dissolved in $CDCl_3$ (3 mL), and the solution was stirred at room temperature for 7 days. All volatiles were removed under reduced pressure (3×10^{-2} mbar). The residue was purified by column chromatography at −10 °C (Al_2O_3, h = 2 cm, $\varnothing$ = 4.5 cm, petroleum ether/Et_2O, stepwise gradient, 1:0–0:1). Evaporation of the first fraction gave product **8** as a colorless solid, which was recrystallized from Et_2O and THF at −50 °C. Single crystals suitable for X-ray study were obtained from a saturated Et_2O solution (185 mg, 0.49 mmol, 18%). M.p. 130 °C; ^{1}H NMR (300.13 MHz, $CDCl_3$, 25 °C, TMS): δ = 1.1 (s, 12H, CH_3), 1.5 (s, 6H, CH_2-C(CH_3)$_2$ and CH_2-CH_2-CH_2), 7.4–7.5 (m, 6H, H_{Ph}), 7.8–8.0 ppm (m, 4H, H_{Ph}); ^{13}C{^{1}H} NMR (75.48 MHz, $CDCl_3$, 25 °C, TMS): δ = 17.4 (s, CH_2-CH_2-CH_2), 24.7 (br s, CH_3), 34.4 (br s, CH_3), 40.7 (s, CH_2-C(CH_3)$_2$), 59.8 (d, $^3J_{P,C}$ = 0.9 Hz, N-C(CH_3)$_2$), 128.4 (d, $^3J_{P,C}$ = 12.4 Hz, *m*-C_{Ph}), 132.0 (d, $^4J_{P,C}$ = 3.3 Hz, *p*-C_{Ph}), 132.0 (d, $^2J_{P,C}$ = 9.4 Hz, *o*-C_{Ph}), 133.3 ppm (d, $^1J_{P,C}$ = 98.1 Hz, *ipso*-C_{Ph}); ^{31}P{^{1}H} NMR (121.51 MHz, $CDCl_3$, 25 °C, H_3PO_4): δ = 38.4 ppm (s_{Sat}, $^1J_{P,C}$ = 98.1 Hz); MS (EI, 70 eV): *m/z* (%): 373 $[M]^{+\bullet}$ (15); elemental analysis calcd (%) for $C_{21}H_{28}NOPS$ (373.49 g mol^{-1}): 67.53, H 7.56, N 3.75, S 8.59; found: C 67.27, H 7.56, N 3.69, S 8.16.

Isolation of ionic phosphane 10

Phosphane sulfide **7** (1.93 g, 5.16 mmol) was dissolved in THF (10 mL), and the solution was heated under stirring at 60 °C for 4 days. All volatiles were removed under reduced pressure (3×10^{-2} mbar). The residue was purified by column chromatography (SiO_2, h = 2 cm, $\varnothing$ = 4.5 cm, petroleum ether/Et_2O, stepwise gradient, 1:0–0:1). Evaporation of the first fraction gave product **10** as a colorless solid, which was recrystallized from THF and *n*-pentane at −30 °C. Single crystals that were suitable for X-ray study were obtained from saturated Et_2O solution (445 mg, 1.19 mmol, 23%). M.p. 178 °C; ^{1}H NMR (300.13 MHz, $CDCl_3$, 25 °C, TMS): δ = 1.4 (s, 12H, CH_3), 1.4–1.6 (br m, 6H, CH_2-C(CH_3)$_2$ and CH_2-CH_2-CH_2), 7.2–7.3 (m, 6H, H_{Ph}), 7.8–7.9 (m, 4H, H_{Ph}), 8.9 ppm (br s, 2H, NH_2); ^{13}C{^{1}H} NMR (75.48 MHz, $CDCl_3$, 25 °C, TMS): δ = 16.5 (s, CH_2-CH_2-CH_2), 27.8 (s, CH_3), 35.1 (s, CH_2-C(CH_3)$_2$), 56.5 (s, N-C(CH_3)$_2$), 127.5 (d, $^3J_{P,C}$ = 12.2 Hz, *m*-C_{Ph}), 129.3 (d, $^4J_{P,C}$ = 2.8 Hz, *p*-C_{Ph}), 130.8 (d, $^2J_{P,C}$ = 10.4 Hz, *o*-C_{Ph}), 143.3 ppm (d, $^1J_{P,C}$ = 103.3 Hz, *ipso*-C_{Ph}); ^{31}P{^{1}H} NMR (121.51 MHz, $CDCl_3$, 25 °C, H_3PO_4): δ = 52.1 ppm (s_{Sat}, $^1J_{P,C}$ = 103.3 Hz); MS (ESI positive): *m/z* (%): 142 $[TMP-H_2]^+$; MS (ESI negative): *m/z* (%): 217 $[Ph_2P(S)]^-$; elemental analysis calcd (%) for $C_{21}H_{30}NOPS$ (375.51 g mol^{-1}): C 61.17, H 8.05, N 3.73, S 8.54; found: C 66.91, H 7.64, N 3.74, S 8.69.

Synthesis of phosphane borane complex 13

A solution of *n*BuLi (1.6 M, 3.5 mL, 5.5 mmol; *n*-hexane) was added slowly to a stirring solution of diphenylphosphane borane complex **12** (1 g, 5 mmol) in toluene (20 mL) at −90 °C. After warming to −40 °C in 1 hour, a solution of TEMPO (1.57 g, 10 mmol) in toluene (5 mL) was added. After 16 h, all volatiles were removed under reduced pressure (3×10^{-2} mbar). The residue was purified by

column chromatography at −10 °C (SiO_2, $h = 5$ cm, $\varnothing = 4.5$ cm, petroleum ether/Et_2O, 20:1–10:1). Evaporation of the first fraction gave product **13** as a colorless solid, which was recrystallized from toluene at −60 °C. Single crystals that were suitable for X-ray study were obtained from a saturated Et_2O solution (740 mg, 2.9 mmol, 58%). M.p. 128 °C; $^1H\{^{11}B\}$ NMR (300.13 MHz, $CDCl_3$, 25 °C, TMS): $\delta =$ 1.0 (s, 6H, CH_3), 1.2 (s, 6H, CH_3), 1.3 (s, 3H, BH_3), 1.3 (s, 1H, CH_2-CH_2-CH_2), 1.4–1.5 (m, 2H, CH_2-$C(CH_3)_2$), 1.6–1.7 (m, 3H, CH_2-$C(CH_3)_2$ and CH_2-CH_2-CH_2), 7.3–7.4 (m, 6H, H_{Ph}), 7.8–8.0 ppm (m, 4H, H_{Ph}); $^{11}B\{^1H\}$ NMR (96.30 MHz, $CDCl_3$, 25 °C, $BF_3{\cdot}OEt_2$): $\delta = -39.6$ ppm (d, $^1J_{P,B} = 63.6$ Hz); ^{11}B NMR (96.30 MHz, $CDCl_3$, 25 °C, $BF_3{\cdot}OEt_2$): $\delta = -39.6$ ppm (qd, $^1J_{B,H} = 95.5$ Hz, $^1J_{P,B} = 63.6$ Hz); $^{13}C\{^1H\}$ NMR (75.48 MHz, $CDCl_3$, 25 °C, TMS): $\delta = 16.9$ (s, CH_2-CH_2-CH_2), 20.6 (s, CH_3), 33.4 (s, CH_3), 40.3 (s, CH_2-$C(CH_3)_2$), 61.7 (d, $^3J_{P,C} = 2.7$ Hz, N-$C(CH_3)_2$), 128.5 (d, $^3J_{P,C} = 10.1$ Hz, *m*-C_{Ph}), 131.1 (d, $^2J_{P,C} = 10.1$ Hz, *o*-C_{Ph}), 131.1 (d, $^4J_{P,C} = 2.4$ Hz, *p*-C_{Ph}), 134.9 ppm (d, $^1J_{P,C} = 63.1$ Hz, *ipso*-C_{Ph}); $^{31}P\{^1H\}$ NMR (121.51 MHz, $CDCl_3$, 25 °C, H_3PO_4): $\delta = 108.9$ (br d, $^1J_{P,B} = 76.7$ Hz); IR (neat): $\tilde{\nu} = 2437$ (w), 2404 (w), 2348 cm^{-1} (w); MS (EI, 70 eV): *m/z* (%): 354 $[M-H]^{+\bullet}$ (2); elemental analysis calcd (%) for $C_{21}H_{31}BNOP$ (355.27 g mol^{-1}): C 71.00, H 8.08, N 3.94; found: C 71.18, H 8.23, N 3.83.

Acknowledgements

We are grateful to the Deutsche Forschungsgemeinschaft (SFB 813 "Chemistry at Spin Centers") and the cost action cm1302 "Smart Inorganic Polymers" (SIPs) for financial support; G.S. thanks Prof. A. C. Filippou for support.

Keywords: density functional calculations · EPR spectroscopy · nitroxyl · TEMPO · phosphanes

[1] Review: L. Tebben, A. Studer, *Angew. Chem. Int. Ed.* **2011**, *50*, 5034–5068; *Angew. Chem.* **2011**, *123*, 5138–5174, and literature cited therein.
[2] a) W. A. Braunecker, K. Matyjaszewski, *Prog. Polym. Sci.* **2007**, *32*, 93–146; b) D. A. Shipp, *Polym. Rev.* **2011**, *51*, 99–103; c) C. J. Hawker, A. W. Bosman, E. Harth, *Chem. Rev.* **2001**, *101*, 3661–3688; d) J. Nicolas, Y. Guillaneuf, C. Lefay, D. Bertin, D. Gigmes, B. Charleux, *Prog. Polym. Sci.* **2013**, *38*, 63–235.
[3] A. Studer, *Chem. Soc. Rev.* **2004**, *33*, 267–273.
[4] a) For Group 13 metals (Al, Ga) see: C. Jones, R. P. Rose, *New J. Chem.* **2007**, *31*, 1484–1487; b) for Group 14 metals (Si, Ge, Sn) see: M. Lucarini, E. Marchesi, G. F. Pedulli, C. J. Chatgilialoglu, *J. Org. Chem.* **1998**, *63*, 1687–1693; c) for Group 15 elements (Sb, Bi) see: S. Ishida, F. Hirakawa, K. Furukawa, K. Yoza, T. Iwamoto, *Angew. Chem. Int. Ed.* **2014**, *53*, 11172–11176; *Angew. Chem.* **2014**, *126*, 11354–11358.
[5] The reaction of Ph_2PH with TEMPO was already described, and compound **2** was proposed as an intermediate, but no evidence provided: R. J. Baker, E. Hashem, *Helv. Chim. Acta* **2010**, *93*, 1081–1085.
[6] a) H. G. Ang, K. K. So, *J. Fluorine Chem.* **1985**, *27*, 451–460; b) M. R. Banks, R. F. Hudson, *J. Chem. Soc. Perkin Trans. 2* **1989**, 463–467 (here, no comment on the homolysis was made); c) F. Gao, K. Auclair, *Phosphorus Sulfur Silicon Relat. Elem.* **2006**, *181*, 159–165.
[7] The P^{III} molecule with a 2-azaadamantane-1-oxyl (AZADO) moiety could be observed in NMR spectra at −40 °C: S. Ishida, F. Hirakawa, T. Iwamoto, *Chem. Lett.* **2015**, *44*, 94–96.
[8] For studies on phosphinoyl radicals, see: a) J. E. Baxter, R. S. Davidson, H. J. Hageman, T. Overeem, *Makromol. Chem. Rapid Commun.* **1987**, *8*, 311–314; b) M. Kamachi, K. Kuwata, T. Sumiyoshi, W. Schnabel, *J. Chem. Soc. Perkin Trans. 2* **1988**, 961–965; c) G. W. Sluggett, C. Turro, M. W. George, I. V. Koptyug, N. J. Turro, *J. Am. Chem. Soc.* **1995**, *117*, 5148–5153; d) U. Kolzcak, G. Rist, K. Dietlicker, J. Wirz, *J. Am. Chem. Soc.* **1996**, *118*, 6477–6489.
[9] P. W. Siu, S. C. Serin, I. Krummenacher, T. W. Hey, D. P. Gates, *Angew. Chem. Int. Ed.* **2013**, *52*, 6967–6970; *Angew. Chem.* **2013**, *125*, 7105–7108.
[10] a) V. Nesterov, S. Schwieger, G. Schnakenburg, S. Grimme, R. Streubel, *Organometallics* **2012**, *31*, 3457–3459; b) V. Nesterov, Z.-W. Qu, G. Schnakenburg, S. Grimme, R. Streubel, *Chem. Commun.* **2014**, *50*, 12508–12511.
[11] Phosphane oxide **4** was already described here: C. Popovici, P. Oña-Burgos, I. Fernández, L. Roces, S. García-Granda, M. J. Iglesias, F. L. Ortiz, *Org. Lett.* **2010**, *12*, 428–431.
[12] Described as trapping product and characterized by ^1H NMR and MS: see Ref. [8a].
[13] J. M. Tao, J. P. Perdew, V. N. Staroverov, G. E. Scuseria, *Phys. Rev. Lett.* **2003**, *91*, 146401.
[14] S. Grimme, J. Antony, S. Ehrlich, H. Krieg, *J. Chem. Phys.* **2010**, *132*, 154104.
[15] S. Grimme, L. Goerigk, *J. Comput. Chem.* **2011**, *32*, 1456–1465.
[16] A. Schäfer, C. Huber, R. Ahlrichs, *J. Chem. Phys.* **1994**, *100*, 5829–5835.
[17] F. Weigend, M. Häser, H. Patzelt, R. Ahlrichs, *Chem. Phys. Lett.* **1998**, *294*, 143–152.
[18] F. Weigend, R. Ahlrichs, *Phys. Chem. Chem. Phys.* **2005**, *7*, 3297–3305.
[19] P. Grace, *J. Am. Chem. Soc.* **1960**, *82*, 4751.
[20] K. E. Debruin, S. M. Schelble, E. E. Boros, *Phosphorus Sulfur Silicon Relat. Elem.* **1993**, *75*, 151–154.
[21] S. Min, H. Ishihara, T. Murai, S. Kato, *Z. Naturforsch. B* **1989**, *44*, 153–157.
[22] a) B. Maillard, K. U. Ingold, *J. Am. Chem. Soc.* **1976**, *98*, 520–523; b) W. C. Danen, D. D. Newkirk, *J. Am. Chem. Soc.* **1976**, *98*, 516–520; c) N. Bricklebank, A. Pryke, *J. Chem. Soc. Perkin Trans. 1* **2002**, 2048–2051.
[23] F. Dornhaus, M. Bolte, H.-W. Lerner, M. Wagner, *Eur. J. Inorg. Chem.* **2006**, 1777–1785.
[24] R. Ahlrichs, M. Bär, M. Häser, H. Horn, C. Kölmel, *Chem. Phys. Lett.* **1989**, *162*, 165–169.
[25] R. Ahlrichs, M. K. Armbruster, R. A. Bachorz, M. Bär, H.-P. Baron, R. Bauernschmitt, F. A. Bischoff, S. Böcker, N. Crawford, P. Deglmann, F. D. Sala, M. Diedenhofen, M. Ehrig, K. Eichkorn, S. Elliott, F. Furche, A. Glöß, F. Haase, M. Häser, C. Hättig, A. Hellweg, S. Höfener, H. Horn, C. Huber, U. Huniar, M. Kattannek, W. Klopper, A. Köhn, C. Kölmel, M. Kollwitz, K. May, P. Nava, C. Ochsenfeld, H. Öhm, M. Pabst, H. Patzelt, D. Rappoport, O. Rubner, A. Schäfer, U. Schneider, M. Sierka, D. P. Tew, O. Treutler, B. Unterreiner, M. von Arnim, F. Weigend, P. Weis, H. Weiss, N. Winter in TURBOMOLE v6.4, TURBOMOLE GmbH, **2012**.
[26] K. Eichkorn, F. Weigend, O. Treutler, R. Ahlrichs, *Theor. Chem. Acc.* **1997**, *97*, 119–124.
[27] P. Deglmann, K. May, F. Furche, R. Ahlrichs, *Chem. Phys. Lett.* **2004**, *384*, 103–107.

Received: December 4, 2015
Published online on ■■ ■■, 0000

FULL PAPER

Phosphanes

T. Heurich, Z.-W. Qu, S. Nožinović, G. Schnakenburg, H. Matsuoka, S. Grimme, O. Schiemann,* R. Streubel**

■■ – ■■

Synthesis and Rearrangement of *P*-Nitroxyl-Substituted P^{III} and P^{V} Phosphanes: A Combined Experimental and Theoretical Case Study

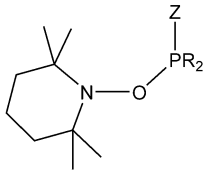

P^{III} and P^{V} *P*-TEMPO phosphanes were synthesized and their behavior in solution were studied. The formation of these complexes was investigated by EPR spectroscopy and NMR kinetic experiments, and DFT calculations provide insights into the formation and decomposition pathways, which involve various open-shell species.